BIOLOGY OF REPRODUCTION **82,** 991–999 (2010)
Published online before print 3 February 2010.
DOI 10.1095/biolreprod.109.081513

Constitutive Activation of Smoothened Leads to Female Infertility and Altered Uterine Differentiation in the Mouse[1]

Heather L. Franco,[3] Kevin Y. Lee,[3] Cory A. Rubel,[3] Chad J. Creighton,[5] Lisa D. White,[4] Russell R. Broaddus,[7] Michael T. Lewis,[6] John P. Lydon,[3] Jae-Wook Jeong,[3] and Francesco J. DeMayo[2,3]

Department of Molecular and Cellular Biology,[3] Department of Molecular and Human Genetics,[4] The Dan L. Duncan Cancer Center,[5] and The Lester and Sue Smith Breast Center,[6] Baylor College of Medicine, Houston, Texas
Department of Pathology,[7] University of Texas M.D. Anderson Cancer Center, Houston, Texas

ABSTRACT

Previous work has identified Indian hedgehog (*Ihh*) as a major mediator of progesterone signaling during embryo implantation. *Ihh* acts through its downstream effector smoothened (*Smo*) to activate the GLI family of transcription factors. In order to gain a better understanding of *Ihh* action during embryo implantation, we expressed a Cre-recombinase-dependent constitutively activated SMO in the murine uterus using the $Pgr^{tm2(cre)Lyd}$ (PR^{cre}) mouse model [$Pgr^{tm2(cre)Lyd+}Gt(ROSA)26Sor^{tm1(Smo/EYFP)Amc+}$ ($PR^{cre/+}SmoM2^{+}$)]. Female $PR^{cre/+}SmoM2^{+}$ mice were infertile. They exhibited normal serum progesterone levels and normal ovulation, but their ova failed to be fertilized in vivo and their uterus failed to undergo the artificially induced decidual response. Examination of the $PR^{cre/+}SmoM2^{+}$ uteri revealed numerous features such as uterine hypertrophy, the presence of a stratified luminal epithelial cell layer, a reduced number of uterine glands, and an endometrial stroma that had lost its normal morphologic characteristics. Microarray analysis of 3-mo-old $PR^{cre/+}SmoM2^{+}$ uteri demonstrated a chondrocytic signature and confirmed that constitutive activation of $PR^{cre/+}SmoM2^{+}$ increased extracellular matrix production. Thus, constitutive activation of *Smo* in the mouse uterus alters postnatal uterine differentiation which interferes with early pregnancy. These results provide new insight into the role of Hedgehog signaling during embryo implantation.

differentiation, implantation, mouse, smoothened, uterus

INTRODUCTION

Uterine development begins at E11.5 (Embryonic Day 11.5) in mice when an invagination of the mesenephros forms the Müllerian duct [1]. After Wolffian duct regression, development continues as the Müllerian duct forms the oviduct, uterus, and vagina. The uterus then differentiates to form two compartments: the myometrium and the endometrium. The endometrium is composed of the luminal and glandular epithelium and the fibroblastic stroma. Glandular development in mice initiates on Postnatal Day 5 with epithelial invaginations that eventually form simple tubular glands by adulthood [2]. Histotrophic secretions from the uterine glands have been shown to be necessary for embryo implantation and, thus, a successful pregnancy [2, 3]. Embryo implantation is a complex process consisting of embryo apposition, attachment, and invasion through the luminal epithelium [4]. These events are followed by the proliferation, differentiation, and vascularization of the fibroblastic stroma in a process known as decidualization. Estrogen (E2) and progesterone (P4), acting through their cognate receptors the estrogen receptor (ER) and the progesterone receptor (PR), mediate these changes in the uterine architecture through the actions of their target genes. One gene identified as being regulated by P4 signaling in the murine uterus is Indian hedgehog (*Ihh*) [5, 6].

Ihh is a member of the mammalian Hedgehog (Hh) family of morphogens [7]. In the absence of Hh, its receptor patched 1 (*Ptch1*) represses the activity of the seven-span transmembrane protein smoothened (SMO). Upon Hh binding to PTCH1, this repression is removed and SMO activates the GLI family of transcription factors to initiate the transcription of Hh target genes, such as *Ptch1*, GLI-Kruppel family member 1 (*Gli1*), and chicken ovalbumin upstream promoter transcription factor II (COUP-TFII, official symbol, *Nr2f2*) [7–9]. Loss of Hh signaling results in embryonic lethality and multiple developmental defects whereas activation of Hh signaling has been implicated in various diseases, such as basal cell carcinoma, medulloblastoma, and rhabdomyosarcoma [7].

Ihh has been shown to play a critical role in bone development [10]. Half of the $Ihh^{-/-}$ mice die prior to birth, but those that survive die at birth due to skeletal abnormalities that do not allow the lungs to expand. Bone development occurs both by intramembranous ossification and endochondral ossification [11]. During endochondral ossification, mesenchymal progenitor cells differentiate into chondrocytes that produce the cartilage matrix, the guide for the future bone. The bone development defect of the $Ihh^{-/-}$ mice was shown to be due to defects in both chondrocyte proliferation and maturation [10]. Furthermore, activation of Hh signaling using either constitutive activation of SMO or overexpression of *Ihh* was sufficient to initiate chondrocyte proliferation [12]. These data suggest that Hh signaling is a major mediator of chondrocyte proliferation and differentiation.

[1]Supported by NIH Grant R01HD042311 (to F.J.D.), NIH Grant R01HD057873 (to J.W.J.), NIH Grant R01CA77530 (to J.P.L.), SPORE in Uterine Cancer NIH P50CA098258 (to R.R.B.), NIH Grant RO1CA127857 (to M.T.L.), NIH Grant P30CA125123 (to C.J.C.), the Reproductive Biology Training Grant 5T32HD07165 and a scholarship from Baylor Research Advocates for Student Scientists (to H.L.F.), the Eunice Kennedy Shriver NICHD/NIH through cooperative agreement U54HD0077495 (to F.J.D.), and U54HD28934 (to the University of Virginia Center for Research in Reproduction Ligand Assay and Analysis Core) as part of the Specialized Cooperative Centers Program in Reproduction and Infertility Research.
[2]Correspondence: Francesco J. DeMayo, Department of Molecular and Cellular Biology, Baylor College of Medicine, Houston, TX 77030. FAX: 713 790 1275; e-mail: fdemayo@bcm.tmc.edu

Received: 17 September 2009.
First decision: 7 October 2009.
Accepted: 25 January 2010.

eISSN: 1529-7268 http://www.biolreprod.org
ISSN: 0006-3363

Ihh has also been shown to play a critical role in uterine function during early pregnancy [13]. When *Ihh* was conditionally ablated in the murine uterus using the $Pgr^{tm2(cre)Lyd}$ (hereafter referred to as PR^{cre}) mouse model, female mice were rendered infertile due to a failure of embryo implantation and an inability to undergo the artificially induced decidual response [14]. This defect was due to an improper preparation of the uterus for the incoming embryo as the uterine stroma exhibited decreased proliferation and reduced vascularization, both of which are necessary for successful embryo implantation and subsequent decidualization [13]. *IHH* may also have a role in the human endometrium as its expression decreases during the transition from the early- to mid-secretory phases when cellular proliferation is reduced [15]. Furthermore, *IHH* was recently identified as a gene that was significantly decreased in women with endometriosis [16]. These data demonstrate a critical role for *Ihh* not only as a mediator of uterine function during pregnancy, but also possibly during the development of uterine diseases, such as endometriosis. Interestingly, the phenotype resulting from *Nr2f2* ablation (either as heterozygotes or by conditional ablation) phenocopies the conditional *Ihh* knockout, further demonstrating a necessary role for Hh signaling during early pregnancy [17, 18].

Therefore, in order to better understand the role of *Ihh* signaling in the uterus, we constitutively activated Hh signaling in the uterus by the expression of a mutant *Smo* allele. Previously, two mutations were identified which lead to constitutive activation of SMO in sporadic basal cell carcinoma: R562Q (SmoM1) and W535L (SmoM2) [19]. One of these mutations, the $Gt(ROSA)26Sor^{tm1(Smo/EYFP)Amc}$ (also known as SmoM2), was used to generate a mouse in which Hh signaling could be activated in a Cre-recombinase-dependent manner [20]. Therefore, we crossed these mice to the PR^{cre} mouse model to constitutively activate SMO in the murine uterus, $Pgr^{tm2(cre)Lyd+}Gt(ROSA)26Sor^{tm1(Smo/EYFP)Amc+}$ (hereafter referred to as $PR^{cre/+}SmoM2^{+}$) [14, 20]. Female $PR^{cre/+}SmoM2^{+}$ mice were found to be infertile due to an inability of the ova to be fertilized in vivo and a failure to undergo the artificially induced decidual response. Furthermore, the $PR^{cre/+}SmoM2^{+}$ uteri exhibited hypertrophy, an abnormal luminal epithelium, and a reduction in the number of uterine glands. The uterine hypertrophy was due to an alteration of the extracellular matrix as demonstrated by both immunohistochemical and microarray analysis. Thus, not only is loss of *Ihh* detrimental to uterine function, but constitutive activation of the Hh-signaling pathway also disrupts normal uterine function as well as postnatal uterine development.

MATERIALS AND METHODS

Animals and Hormone Treatments

Mice were maintained in the designated animal care facility at Baylor College of Medicine according to the institutional guidelines for the care and use of laboratory animals. SmoM2 mice were obtained from Dr. Andrew P. McMahon (Department of Molecular and Cellular Biology, Harvard University, Boston, MA) [20]. The control group includes $PR^{+/+}SmoM2^{-}$, $PR^{cre/+}SmoM2^{-}$ and $PR^{+/+}SmoM2^{+}$ mice. No differences were observed between the three genotypes of the control group. Eight-wk-old female mice were mated to wild-type male mice, and the day of the postcoital plug was designated as Day 0.5. Mice were killed on Day 4.5.

Superovulation was induced in 3-wk-old female mice by administering 5 international units (IU) of equine chronic gonadotropin intraperitoneally (i.p.) (VWR Scientific, West Chester, PA) followed by 5 IU human chorionic gonadotropin (hCG) i.p. (Pregnyl, Organon International, Roseland, NJ) 48 h later at which point they were placed with males. The mice were killed 24 h later, and oocytes were flushed from the oviducts and counted. Blood was collected from 3-mo-old mice, and serum was isolated by centrifugation using serum separator tubes (BD, Franklin Lakes, NJ). The serum was sent to the University of Virginia Center for Research in Reproduction Ligand Assay and Analysis Core for analysis of P4 by radioimmunoassay. In vitro fertilization was performed as previously described [21]. Briefly, female mice were administered superovulatory hormones as described above. The mice were killed 12 h after hCG injection and ova were collected. Sperm (1–2 million) was added 1.5 h later and was incubated for 4 h at 37°C. The number of fertilized and unfertilized ova was assessed 24 h later by their development to the two-cell stage.

The artificial induction of decidualization has been previously described [22]. Briefly, 6-wk-old female mice were ovariectomized and treated with three daily injections of 100 ng E2 per mouse. After 2 days rest, mice were then treated with daily subcutaneous (s.c.) injections of 1 mg P4 and 6.7 ng E2 per mouse for 3 days. Six hours after the last injection, one uterine horn was traumatized by the injection of 50 μl of sesame oil. Mice were given daily s.c. injections of 1 mg P4 and 6.7 ng E2 per mouse following the trauma. Mice were kiled 5 days after the trauma by cervical dislocation while under an anesthetic, Avertin (2,2–tribromoethyl alcohol, Sigma–Aldrich, St. Louis, MO). At the time of dissection, uterine tissues were placed in 4% (vol/vol) paraformaldehyde (PFA) or flash frozen and stored at −80°C.

β-Galactosidase Activity Staining

The expression of *Ptch1* in the uterus was assayed by crossing $Ptch1^{+/-}$ mice into the $PR^{cre/+}SmoM2^{+}$ mice. In the process of ablating *Ptch1*, the *LacZ* gene was inserted into the *Ptch1* locus, which allows us to assay for *Ptch1* expression by β-galactosidase staining (i.e., X-gal staining) [23]. This staining was also used to investigate Cre activation by crossing the PR^{cre} mouse model to the ROSA26-LacZ reporter mouse ($Pgr^{tm2(Cre)Lyd}$ $Gt(ROSA)26Sor^{tm1Sor}$, hereafter referred to as $PR^{cre/+}R26R^{+}$) [24]. In these mice, X-gal staining is indicative of Cre activation. Uteri were fixed in 4% PFA (vol/vol) for 3 h, followed by a sucrose gradient (10%, 15%, and 20% in Hanks balanced salt solution; Invitrogen, Carlsbad, CA) and embedded in optimal-cutting temperature compound. The X-gal staining solution was prepared by dissolving X-gal (Invitrogen, Carlsbad, CA) in dimethylformamide to make a 40 mg/ml solution. A 1 mg/ml solution was prepared by further diluting the X-gal solution in warm tissue stain base solution (Chemicon, Billerica, MA). The sections were cut at 12 μm, postfixed in 4% PFA, and stained with the X-gal staining solution overnight at 37°C. Positive staining is visualized as a blue color, and the counterstaining is nuclear fast red.

Immunohistochemistry

Uteri were fixed overnight in 4% PFA (vol/vol), followed by thorough washing in 70% ethanol; tissues were processed, embedded in paraffin, and sectioned. Uterine sections from paraffin-embedded tissue were cut at 5 μm and mounted on silane-coated slides, deparaffinized, and rehydrated in a graded alcohol series. Sections were preincubated with 10% normal goat serum in PBS (pH 7.5) and then incubated with anti-CD10 (1:100, Novocastra, Newcastle upon Tyne, U.K.), anti-cleaved caspase 3 (1:100, Cell Signaling, Danvers, MA), anti-PR (1:200, DAKO, Carpinteria, CA), or anti-ERα (1:200, DAKO) in 10% normal serum in PBS (pH 7.5). On the following day, sections were washed in PBS and incubated with biotinylated secondary antibody (5 μl/ml; Vector Laboratories, Burlingame, CA) for 1 h at room temperature. Immunoreactivity was detected using the DAB Substrate kit (Vector Laboratories); the immunoreactivity was visualized as brown staining. Slides with no primary antibody were used as a negative control. Proliferation was assessed using the Amersham Cell Proliferation kit (GE Healthcare, Piscataway, NJ) according to manufacturer's instructions. Alcian blue and Masson trichrome staining were performed by the Baylor College of Medicine Center for Comparative Medicine Comparative Pathology Laboratory according to standard protocols.

RNA Isolation and Microarray Analysis

Total RNA was extracted from uterine tissues using the Qiagen RNAeasy total RNA isolation kit (Qiagen, Valencia, CA). The RNA was pooled from the uteri of three mice per genotype. All the RNA samples were analyzed with a Bioanalyser 2100 (Agilent Technologies, Wilmington, DE) before microarray hybridization. The fragmented, labeled cRNA (15 μg) was hybridized to Affymetrix mouse genome 430 2.0 arrays (Affymetrix, Santa Clara, CA) by the Baylor College of Medicine Microarray Core Facility. All the experiments were performed in triplicate with independent pools of RNA. Array data have been deposited in the Gene Expression Omnibus (GEO, GSE17263).

Affymetrix CEL files were processed using dChip (www.dchip.org, PM-MM model, invariant set normalization). Probe sets with average signal of <40

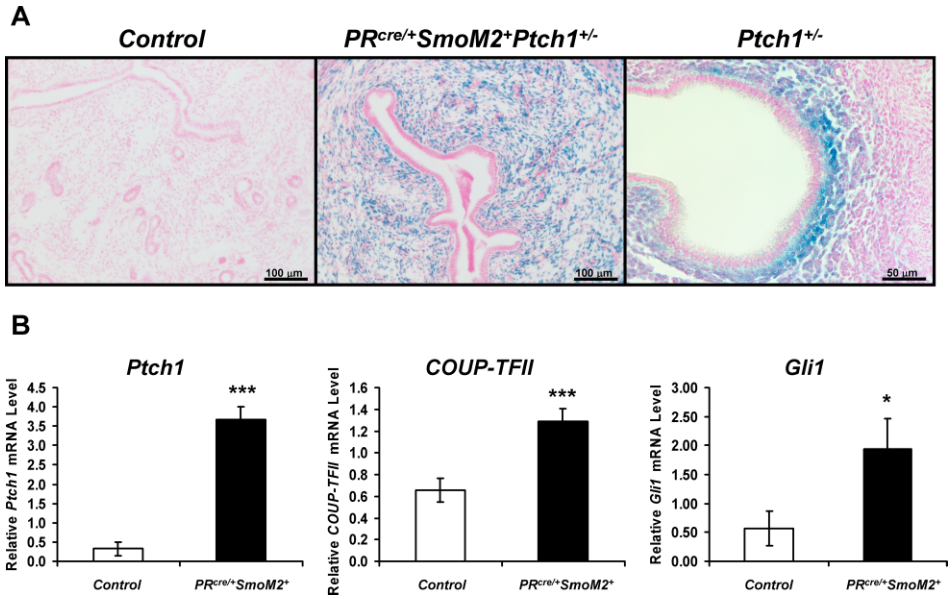

FIG. 1. Generation of mice with constitutive activation of smoothened in the uterus. **A**) X-gal staining of 3-mo-old control (left) and $PR^{cre/+}SmoM2^{+}$ (middle) mice crossed to the *Ptch1-LacZ* reporter mouse that expresses *LacZ* under the control of the *Ptch1* promoter. Normal expression of *Ptch1* on Day 4.5 of pregnancy as observed by X-gal staining of the *Ptch1-LacZ* reporter mouse (right). Blue staining is indicative of PITCH1 expression. Bars = 100 μm (left and middle) and 50 μm (right). **B**) Real-time PCR analysis of the Hh target genes *Ptch1, Nr2f2,* and *Gli1* in 3-mo-old control and $PR^{cre/+}SmoM2^{+}$ uteri (*$P < 0.05$, ***$P < 0.001$; N = 5 mice per genotype, mean ± SEM).

units across profiles were filtered from the analysis. Two-sided *t*-tests and fold changes were carried out as previously described to define differentially expressed genes [25]. Differentially expressed genes were then classified according to Gene Ontology function using Affymetrix annotation (NetAffx; http://affymetrix.com/index.affx), and pathway analysis was performed using DAVID Analysis [26, 27] and Ingenuity Systems Software (Ingenuity Systems, Inc., Redwood City, CA). A two-sided *P*-value cutoff of 0.01 was used to define differentially expressed genes in the Mrugala dataset, and the one-sided Fisher exact test was used to define significance of overlap with the SmoM2-related gene sets (the gene population being the 15092 unique human ortholog genes represented on the mouse 430_2 array).

Real-Time PCR Analysis

Total RNA was extracted from uterine tissues using the Trizol reagent according to manufacturer's instructions (Invitrogen). One μg of the RNA was reverse transcribed into cDNA with M-MLV (Invitrogen) in a 20-μl volume. Expression levels of mRNA were measured by real-time PCR TaqMan analysis using the ABI Prism 7700 Sequence Detector System according to the manufacturer's instructions (PE Applied Biosystems, Foster City, CA). Real-time probes were purchased from Applied Biosystems (Foster City, CA). For a complete list, see Supplemental Table S1 (all the supplemental data are available online at www.biolreprod.org). All real-time PCR was done using independent RNA sets. All mRNA quantities were normalized against 18S RNA using ABI rRNA control reagents, and a no template control was used as a negative control. Statistical analyses used one-way ANOVA followed by Tukey post-hoc multiple range test with the Instat package from GraphPad (San Diego, CA).

RESULTS

Generation of Mice with Constitutive Activation of Smoothened in the Uterus

In order to further understand the role of Hh signaling in the uterus, we generated mice with constitutive activation of SMO in the uterus by crossing SmoM2 mice with the mouse model [14, 20]. These mice have SMO activated in all PR-positive cells, which includes all the compartments of the uterus. In order to determine where activation of Hh signaling occurred in the uterus with expression of the SmoM2 allele, we assayed for the expression of *Ptch1*. Using the *Ptch1-LacZ* reporter mouse (official symbol $Ptch1^{tm1Mps}$ in which *LacZ* is expressed under the control of the *Ptch1* promoter), blue X-gal staining can be seen specifically in the stroma of 3-mo-old $PR^{cre/+}SmoM2^{+}$ uteri but not that of the control uteri, indicating that *Ptch1* is expressed only in the $PR^{cre/+}SmoM2^{+}$ stroma (Fig. 1A) [23]. *Ptch1* expression is normally restricted to the subepithelial stroma just prior to the time of embryo implantation (Fig. 1A). Furthermore, the $PR^{cre/+}SmoM2^{+}$ mice exhibited an increase in the Hh target genes, *Ptch1, Nr2f2,* and *Gli1*, as shown by real-time PCR analysis of 3-mo-old whole uterus (Fig. 1B). Thus, we have successfully generated mice in which SMO is constitutively activated in the stroma of the uterus.

Impact of Constitutive Activation of Smoothened on Female Fertility

In order to determine the effect of constitutive activation of Hh signaling on female fertility, female control and $PR^{cre/+}SmoM2^{+}$ mice were bred to wild-type male mice. During the time of observation, control mice exhibited normal fecundity whereas the $PR^{cre/+}SmoM2^{+}$ mice were found to be infertile (Table 1). These results demonstrate that constitutive activation of Hh signaling is detrimental to female fertility.

Because the PR^{cre} mouse model recombines alleles in multiple reproductive tissues, we first assessed the impact of Hh activation on ovarian function [14]. Therefore, female control and $PR^{cre/+}SmoM2^{+}$ mice were administered super-ovulatory hormones (see *Materials and Methods*) and mated to wild-type male mice (N = 8). The next morning, the number of fertilized and unfertilized ova was examined. Female

TABLE 1. Effect of constitutive activation of Hh signaling on female fertility.

Female genotype	No. of females	No. of pups	No. of litters	Average pups per litter[a]	Average litters per female[a]
Control	6	70	8	8.75 ± 0.75	1.33 ± 0.21
$PR^{cre/+}SmoM2^{+}$	6	0	0	NA	NA

[a] NA, not available.

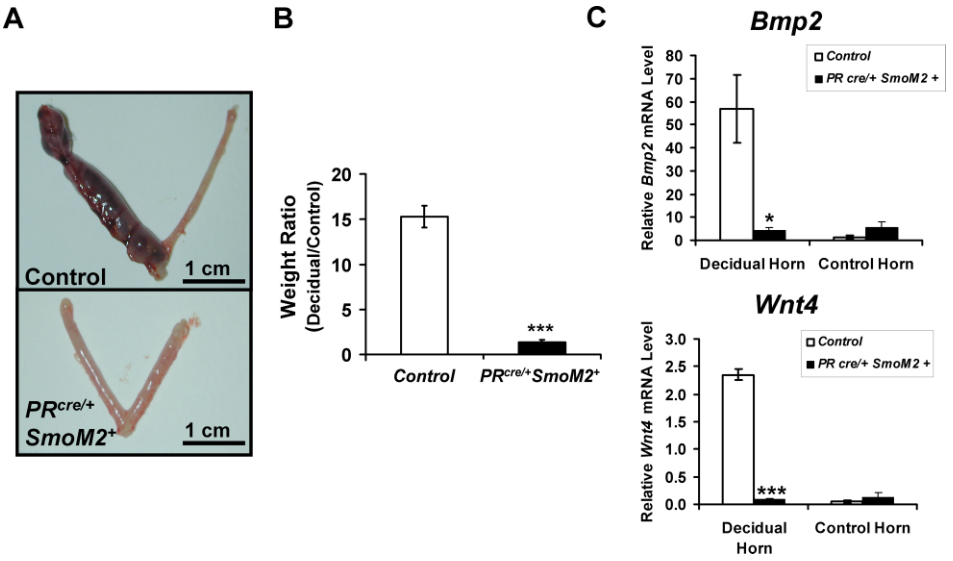

FIG. 2. Female $PR^{cre/+}SmoM2^{+}$ mice fail to undergo the artificial decidual response. **A**) Gross morphology of control and $PR^{cre/+}SmoM2^{+}$ mice artificially stimulated to undergo decidualization. Mice were killed 5 days after the decidual trauma. On the left is the decidual horn and on the right is the control horn. Bars = 1 cm. **B**) Ratio of decidual to control horn weights of the control and $PR^{cre/+}SmoM2^{+}$ mice 5 days after the decidual trauma in the artificial decidual reaction (*$P < 0.05$, N = 5 mice per genotype, mean ± SEM). **C**) Real-time PCR analysis of the decidual markers *Bmp2* and *Wnt4* in both the decidual and control horns of control and $PR^{cre/+}SmoM2^{+}$ mice 5 days after the decidual trauma (***$P < 0.001$, N = 5 mice per genotype, mean ± SEM).

$PR^{cre/+}SmoM2^{+}$ mice were able to ovulate normally with 13.22 ± 2.44 ova ovulated compared to 13.88 ± 3.41 from controls. However, while control mice exhibited a 55.90% ± 18.52% fertilization rate, no fertilized ova were observed in the $PR^{cre/+}SmoM2^{+}$ mice. Examination of the ova revealed that they underwent normal cumulus expansion (data not shown). To determine if the fertilization defect may be due to an intrinsic defect of the ova, we assessed their ability to undergo in vitro fertilization. Ova from $PR^{cre/+}SmoM2^{+}$ mice were able to be fertilized similarly to ova from control mice (13/50 (26.0%) vs. 17/55 (30.9%), respectively; N = 5). Furthermore, serum P4 levels were normal in 3-mo-old $PR^{cre/+}SmoM2^{+}$ mice (6.72 ± 1.00 ng/ml) compared to controls (8.34 ± 3.99 ng/ml). These results suggest that the impaired fertility of the $PR^{cre/+}SmoM2^{+}$ mice is partly due to a fertilization defect that is not due to a deficiency in the ova themselves.

To examine the effect of constitutive activation of SMO on uterine function, female $PR^{cre/+}SmoM2^{+}$ mice were assessed for their ability to undergo the artificially induced decidualization response. Six-wk-old female control and $PR^{cre/+}SmoM2^{+}$ mice were ovariectomized and treated with hormones to mimic pregnancy as previously described (see *Materials and Methods*) [22]. The mice received an injection of oil to mimic the implanting embryo and were killed 5 days later. Control mice responded normally with an increase in the weight of the decidual horn compared to the control horn, however, the $PR^{cre/+}SmoM2^{+}$ mice did not respond to the decidual stimulus (Fig. 2A). These results can be quantified by taking the ratio of the weight of the decidual horn to the control horn. Quantification confirmed the observations of the gross histology (Fig. 2B). Furthermore, the expression of markers of decidualization, bone morphogenetic protein 2 (*Bmp2*) and wingless-related MMTV (mouse mammary tumor virus) integration site 4 (*Wnt4*), were significantly reduced in the decidual horn of the $PR^{cre/+}SmoM2^{+}$ mice compared to controls (Fig. 2C). Thus, independent of the fertilization defect, the uterus displays a striking defect in its ability to undergo stromal cell decidualization.

$PR^{cre/+}SmoM2^{+}$ *Uteri Exhibit Altered Uterine Differentiation*

In order to determine if constitutive activation of Smo affected uterine development, the uteri of control and $PR^{cre/+}SmoM2^{+}$ mice were examined. At 5 mo of age, the $PR^{cre/+}SmoM2^{+}$ uteri were larger than control uteri, demonstrating no change in uterine length but an increase in uterine diameter (Fig. 3A). Examination of the uterine histology revealed no differences in the myometrium of the $PR^{cre/+}SmoM2^{+}$ uteri, but vast differences in the endometrium (Fig. 3, B and C). In lieu of the simple columnar epithelium observed in the control uteri, the $PR^{cre/+}SmoM2^{+}$ uteri exhibited the presence of a second cell layer below the columnar epithelial cells (Fig. 3B). Examination of these cells in 3-mo-old uteri demonstrated that these cells were p63 positive, indicating that they are of a basal cell type (Fig. 3C). None of the control mice displayed the presence of this p63-positive basal cell population. In addition, the mice exhibited a reduction in the number of uterine glands and an increase in size of the uterine stroma. Real-time PCR analysis for forkhead box A2 (*Foxa2*), a protein expressed specifically in the glandular epithelium, further confirmed the reduction in uterine glands as the protein's expression was reduced in the $PR^{cre/+}SmoM2^{+}$ mice compared to controls (Fig. 3D) [28]. To determine the age of onset of these histological features, we examined the histology of $PR^{cre/+}SmoM2^{+}$ uteri at various ages. The PR^{cre} mouse model recombines alleles in the uterine epithelium and stroma at 10 days of age as shown by X-gal staining of the $PR^{cre/+}R26R^{+}$ mice (Supplemental Figure S1) [24]. At this time point, SMO is activated as shown by the blue X-gal staining in the $PR^{cre/+}SmoM2^{+}Ptch^{+/-}$ mice, and this activation occurs specifically in the uterine stroma (Supplemental Figure S1). Therefore, we began examining mice at 1 mo of age to determine the age of onset of the phenotypic consequences resulting from *Smo* activation. No stromal or luminal epithelial defects were apparent at 1 mo and 6 wk of age in the $PR^{cre/+}SmoM2^{+}$ uteri compared to controls (data not shown). However, mice at this age did display a reduction in uterine glands. The stromal and luminal epithelial phenotype of these mice became apparent at 3 mo of age and became more marked with age. Thus, we focused our analysis on 3-mo-old uteri as this appears to be a transition time point.

The increase in stromal size could be explained by an increase in stromal cell proliferation or a decrease in apoptosis. However, immunohistochemical analysis of BrdU (bromodeoxyuridine), a cell proliferation marker, and cleaved caspase 3, an apoptotic marker, showed no difference between control and $PR^{cre/+}SmoM2^{+}$ mice at 3 mo of age (Supplemental Figure S2). Because the change in the uterine stroma was not due to an alteration in stromal cell proliferation or apoptosis, we

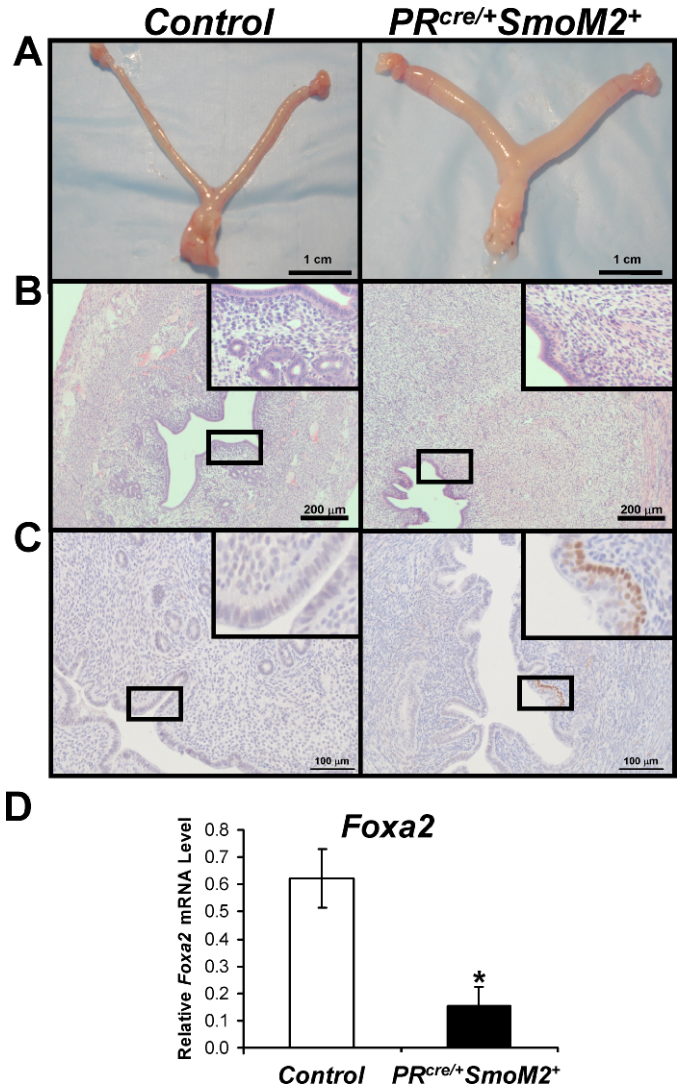

FIG. 3. $PR^{cre/+}SmoM2^{+}$ mice exhibit altered uterine differentiation. **A**) Gross morphology of 5-mo-old control (left) and $PR^{cre/+}SmoM2^{+}$ (right) mice. **B**) Hematoxylin and eosin staining of 5-mo-old control (left) and $PR^{cre/+}SmoM2^{+}$ (right) uteri. **C**) Immunohistochemical analysis of the basal cell marker p63 in 3-mo-old control (left) and $PR^{cre/+}SmoM2^{+}$ (right) uteri. **D**) Real-time PCR analysis of the glandular marker *Foxa2* in 3-mo-old mice ($*P < 0.05$, N = 5 mice per genotype, mean ± SEM). Bars = 1 cm (**A**), 200 μm (**B**), and 100 μm (**C**).

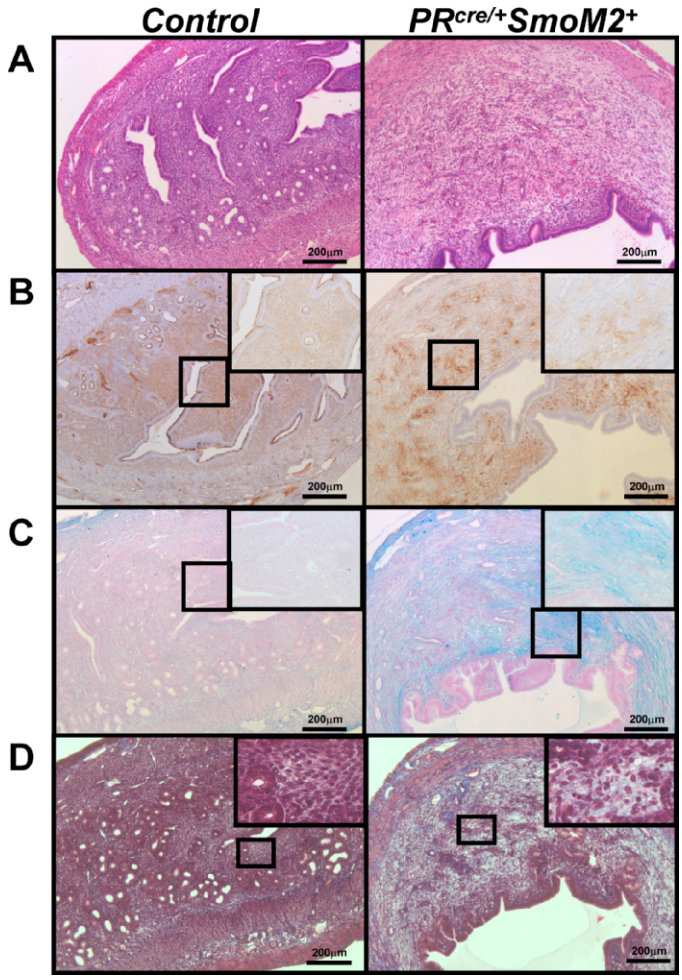

FIG. 4. $PR^{cre/+}SmoM2^{+}$ uteri exhibit altered stromal characteristics. **A**) Hematoxylin and eosin staining of 3-mo-old control (left) and $PR^{cre/+}SmoM2^{+}$ (right) uteri. **B**) Immunohistochemistry for the stromal cell marker CD10 in 3-mo-old control (left) and $PR^{cre/+}SmoM2^{+}$ (right) uteri. Counterstained with hematoxylin. **C**) Alcian blue staining of 3-mo-old control (left) and $PR^{cre/+}SmoM2^{+}$ (right) uteri. **D**) Masson trichrome staining of 3-mo-old control (left) and $PR^{cre/+}SmoM2^{+}$ (right) uteri. Bars = 200 μm.

hypothesized that the phenotype observed may be due to a change in stromal cell differentiation. At 3 mo of age, uterine hypertrophy due to an expansion of the uterine stroma can already be observed in the $PR^{cre/+}SmoM2^{+}$ mice (Fig. 4A). CD10 is a known marker of normal, mature human endometrial stromal cells [29]. To determine if differentiation of the stroma occurred, we stained for CD10. In the control mice, we observed stroma-specific staining of CD10, indicating that it also marks mouse endometrial stromal cells (Fig. 4B). In contrast, the $PR^{cre/+}SmoM2^{+}$ mice exhibited a decrease in CD10 stromal staining. Thus, constitutive activation of SMO in the uterus alters the characteristics of the uterine stroma.

Since endometrial stromal cells exhibit reduced expression of the stromal cell marker CD10, we surveyed the stromal cells for the expression of other cell type-specific markers to determine if activation of SMO altered endometrial stromal differentiation. Uteri were assessed for their ability to differentiate into fat, muscle, or chondrocytes by oil-red-O staining, immunohistochemical analysis for smooth muscle alpha actin, or Alcian blue staining, respectively. There was no difference in oil-red-O staining or smooth muscle alpha actin levels between the control and $PR^{cre/+}SmoM2^{+}$ uteri indicating that the stromal cells were not differentiating into either fat or muscle (data not shown). Rather, the $PR^{cre/+}SmoM2^{+}$ uteri stained positive for Alcian blue, a marker of mucopolysaccharides and glycosaminoglycans (Fig. 4C). These results suggested an alteration of extracellular matrix components. Therefore, we performed periodic acid Schiff (PAS) and Masson trichrome staining. The $PR^{cre/+}SmoM2^{+}$ uteri were PAS-negative, demonstrating that there was not an expansion of glycogen in these uteri (data not shown). However, there was increased collagen staining in the $PR^{cre/+}SmoM2^{+}$ uteri as evidence by blue staining in the Masson trichrome staining (Fig. 4D). The Masson trichrome staining also confirmed that there was no alteration in the muscle content of the $PR^{cre/+}SmoM2^{+}$ uteri (red staining). Thus, the expansion of the $PR^{cre/+}SmoM2^{+}$ stroma is due to an alteration in the extracellular matrix.

Microarray Analysis of the $PR^{cre/+}SmoM2^{+}$ *Uteri*

In order to determine the mechanism by which SMO regulates the extracellular matrix, high-density DNA microarray analysis was performed on 3-mo-old control and $PR^{cre/+}SmoM2^{+}$ uteri. Total RNA extracts were subjected to microarray analysis using the Affymetrix mouse genome 430 2.0 arrays. This analysis revealed 1383 and 1260 Affymetrix probe sets (each representing a gene transcript) with abundances significantly increased or decreased, respectively, in the $PR^{cre/+}SmoM2^{+}$ uterus compared to controls ($P < 0.01$, fold change >1.5). A complete list of the genes increased and decreased can be found in Supplemental Tables S2 and S3, respectively. Pathway analysis using DAVID Analysis and Ingenuity Systems Software revealed a number of pathways regulated by Hh activation, including, but not limited to, WNT signaling, vitamin D activation, cell communication, tight junction signaling, and IGF1 (insulin-like growth factor 1) signaling (Supplemental Table S4) [26, 27].

Because of the established role of Hh signaling in chondrocyte proliferation and differentiation [10, 12] and the increased staining of extracellular matrix markers in the $PR^{cre/+}SmoM2^{+}$ uteri, we decided to compare our array list to results of an array dataset from Mrugala et al. in which mesenchymal stem cells were induced to form chondrocytes by treatment with either BMP2 or transforming growth factor beta 2 (TGFB2) [30]. This analysis demonstrated that there was significant overlap between the results of the Mrugala dataset and our dataset, which indicated that the $PR^{cre/+}SmoM2^{+}$ uteri were expressing a chondrocytic signature (Supplemental Table S5). Of the 914 distinct human orthologs of genes increased in the $PR^{cre/+}SmoM2^{+}$ uteri, 51 were BMP2-induced and 37 were TGFB2-induced at 21 days in the Mrugala dataset ($P < 5E{-}5$ and $P < 0.01$, respectively, one-sided Fisher exact test). Of the 819 human orthologs decreased in the $PR^{cre/+}SmoM2^{+}$ uteri, 34 were BMP2-repressed and 34 were TGFB2-repressed ($P < 0.01$ for each, one-sided Fisher exact test). Furthermore, we also compared our array list to genes found specifically in cartilage [31]. Again, there were a number of genes that overlapped between the two gene lists with 13 genes in the $PR^{cre/+}SmoM2^{+}$ microarray data set identified as cartilage specific (Supplemental Table S6). To confirm these results, real-time PCR analysis was performed on some of the identified genes. Both *Bmp2* and wingless-related MMTV integration site 5A (*Wnt5a*), another known inducer of chondrocyte differentiation [32], were increased in the $PR^{cre/+}SmoM2^{+}$ uteri compared to controls (Fig. 5A). In addition, members of the parathyroid hormone-signaling pathway (*Pthlh*/*Pthrp* and *Pthr1*) were significantly increased in the $PR^{cre/+}SmoM2^{+}$ uteri (Fig. 5A). This signaling pathway has previously been shown to act downstream of *Ihh* in bone formation, suggesting that its induction in the $PR^{cre/+}SmoM2^{+}$ uterus may explain the observed phenotype [33]. The expression of genes induced during chondrocyte differentiation—collagen 11α1 (*Col11α1*), laminin alpha 2 (*Lama2*), nidogen 1 (*Nid1*), cartilage-associated protein (*Crtap*)—or identified as cartilage specific—podoplanin (*Pdpn*), hyaluron synthase 2 (*Has2*), collagen 11α1 (*Col11α1*)—were significantly increased in the SmoM2 uteri (Fig. 5B). Furthermore, the extracellular matrix components bigylcan (*Bgn*) and fibromodulin (*Fmod*) were also found to be increased in the $PR^{cre/+}SmoM2^{+}$ uteri (Fig. 5B). These results confirm that there is an alteration of the extracellular matrix upon constitutive activation of Smo in the uterus.

Nonuterine Phenotype Observed in the SmoM2

The only nonuterine phenotype observed in the $PR^{cre/+}SmoM2^{+}$ mice was the presence of upper body tumors (Supplemental Figure S3). These tumors were located in the muscle surrounding the mammary gland and resembled rhabdomyosarcomas that have been previously associated with activation of Hh signaling [34–37]. Although the focus of this study is to assay the impact of $PR^{cre/+}SmoM2^{+}$ expression on the uterus, the presence of these tumors limited our study of the uterus as we were only able to observe mice until they reached 5 mo of age.

DISCUSSION

Previously, we demonstrated that the Hh-signaling pathway is critical for uterine function as conditional ablation of *Ihh* in the uterus rendered female mice infertile due to an inability of embryo attachment and subsequent decidualization [13]. In order to further understand the role of Hh signaling during embryo implantation, we constitutively activated SMO in the uterus using the PR^{cre} mouse model [14]. The PR^{cre} mouse model recombines alleles in all PR-positive cells, which includes the mammary gland, pituitary, corpus luteum of the ovary, and all compartments of the uterus [14]. Stroma-specific activation of SMO was verified by stroma-specific activation of the *Ptch1* promoter as evidence by the *Ptch1-LacZ* reporter mice (Fig. 1A). This expression occurred throughout the stromal compartment that is in contrast to normal activation, which occurs only in the subepithelial stroma. Furthermore, Hh target genes were significantly increased in the $PR^{cre/+}SmoM2^{+}$ uteri (Fig. 1B). Therefore, we successfully generated mice with SMO activation in the uterus. The limited expression of SmoM2 in the uterine stroma may be due to inefficient recombination of this particular allele in the luminal epithelium, inefficient expression of the SmoM2 transgene after activation, or a lack of the ability of luminal epithelial cells to support signaling downstream of *Smo*.

Constitutive activation of SMO resulted in female mice that were infertile due to the inability of ova to be fertilized in vivo and the lack of the uterus to undergo a decidual response. Female $PR^{cre/+}SmoM2^{+}$ mice exhibited normal ovulation in response to superovulatory hormones. These ova exhibited normal cumulus expansion which is in contrast to the $Amhr2^{cre/+}SmoM2$ (official symbol $Amhr2^{tm3(cre)Bhr}$ $Gt(ROSA)26Sor^{tm1(Smo/EYFP)Amc+}$) mice that exhibited a defect in cumulus expansion [38]. This discrepancy can be potentially explained by the activation of the SmoM2 allele late in folliculogenesis in the $PR^{cre/+}SmoM2^{+}$ mouse at which point SMO activation has no effect on folliculogenesis. In addition, normal serum P4 levels were observed in the $PR^{cre/+}SmoM2^{+}$ mice compared to controls. These data suggest that ovarian function was unaffected in these mice.

Interestingly, fertilization of the ova in the $PR^{cre/+}SmoM2^{+}$ mice did not occur. As the ova were able to be fertilized in vitro, this suggests that the defect is not due to an intrinsic defect in the ova themselves, but may be due to a defect in sperm transport as a result of the altered uterine morphology of the $PR^{cre/+}SmoM2^{+}$ mice. In mice, sperm is initially deposited in the vagina at which point it is quickly transported through the cervix to the uterus [39]. Once in the uterus, sperm is transported to the oviduct through the combined actions of myometrial contractions, cervical mucosal flow, and the actions of mucins and glycoproteins that line the uterine lumen. The entrance of sperm to the uterine cavity triggers an immune response highlighted by an infiltration of leukocytes that could destroy the sperm, demonstrating the importance of

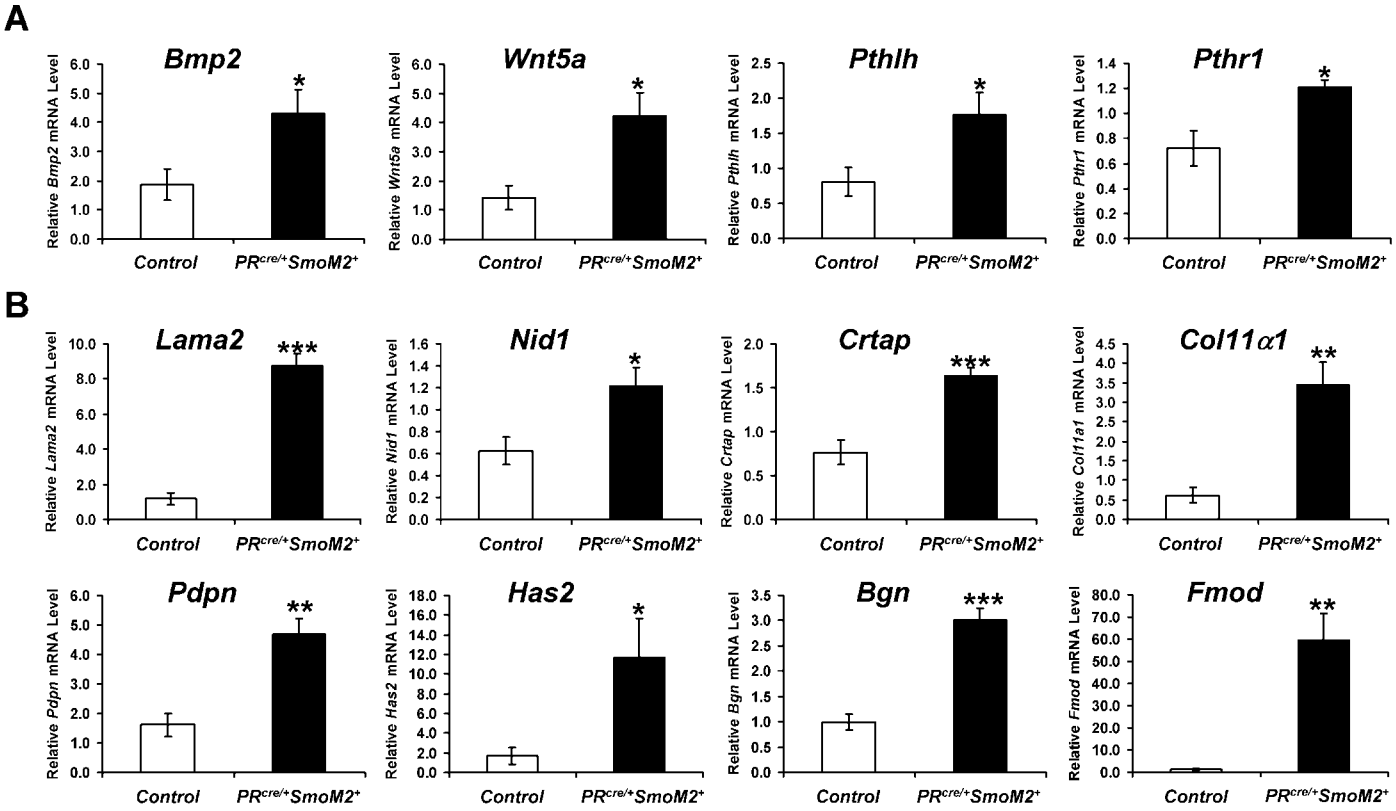

FIG. 5. $PR^{cre/+}SmoM2^{+}$ mice exhibit an increase in extracellular matrix components. **A**) Real-time PCR analysis of the inducers of chondrocyte differentiation, *Bmp2* and *Wnt5a,* and members of the parathyroid hormone-signaling pathway, *Pthlh* and *Pthr1*. **B**) Real-time PCR analysis of genes induced, including those of chondrocyte differentiation (*Col11α1, Lama2, Nid1, Crtap*), cartilage-specific genes (*Pdpn, Has2, Col11α1*), or extracellular matrix components (*Bgn, Fmod*) (*$P < 0.05$, **$P < 0.01$, ***$P < 0.001$; N = 5 mice per genotype, mean ± SEM).

efficient sperm transport from the site of deposition to the site of fertilization. Because of the drastic changes observed in the $PR^{cre/+}SmoM2^{+}$ uteri, any of these steps in sperm transport could be affected by Hh activation resulting in no fertilization. Therefore, further investigation needs to be done to determine if any of these actions are altered by Smo activation that results in the defect in fertilization.

In order to assess the functionality of the uterus, female $PR^{cre/+}SmoM2^{+}$ mice were assessed for their ability to undergo the artificial decidual response. While control mice exhibited a normal increase in size and weight of the decidual horn, $PR^{cre/+}SmoM2^{+}$ mice failed to achieve any response, which was confirmed by the lack of expression of the decidual markers *Bmp2* and *Wnt4* (Fig. 2). Since conditional ablation of *Ihh* and constitutive activation of SMO both result in a lack of a decidual response, this suggests that the level of Hh signaling must be tightly regulated in the uterus in order for a successful pregnancy to occur. In addition to the possible intrinsic defect in the uterine stromal cells, the lack of a decidual response may also be due to the reduction in the number of uterine glands in the $PR^{cre/+}SmoM2^{+}$ uteri (Fig. 3B). Uterine glands have been shown to be critical for embryo implantation as they secrete factors necessary for survival of the embryo [2, 3]. One such factor is leukemia inhibitory factor (*Lif*). LIF is produced by the uterine glands and has been shown to be critical for embryo implantation as female $Lif^{-/-}$ mice fail to achieve successful embryo implantation [40]. Furthermore, the uteri are unable to undergo the artificially induced decidual response [41]. Thus, secretions from the uterine glands are critical for successful embryo implantation and subsequent decidualization.

The diminished number of uterine glands in the $PR^{cre/+}SmoM2^{+}$ mice may provide insight into the regulation of uterine gland development. Glandular development in the mouse initiates on Postnatal Day 5 with the invagination and budding of the luminal epithelium [2]. This budding persists until around Postnatal Day 15 when the presence of simple tubular glands can be observed. While little is known about the regulation of gland development in mice, administration of the progestin norgestomet in neonatal sheep inhibits gland formation [42]. These data suggest that inappropriate P4 signaling is detrimental to gland formation in sheep. In the $PR^{cre/+}SmoM2^{+}$ uterus, there is a reduction in the number of uterine glands (Fig. 3). Because *Ihh* is a P4-regulated gene, activation of Hh signaling using the SmoM2 allele may lead to inappropriate P4 signaling and thus inhibition of glandular formation in the mouse as in the sheep. This appears to occur independent of an alteration in steroid hormone receptor levels as both PR and ER levels were unaffected by SMO activation (Supplemental Figure S4). Interestingly, as SMO activation was only observed in the stroma, this suggests that the uterine stroma acts on the epithelium to regulate glandular development. Identification of the paracrine factor necessary for this regulation will be critical to understand the mechanism of endometrial glandular development.

In addition to the reduction in uterine glands, female $PR^{cre/+}SmoM2^{+}$ mice exhibit uterine hypertrophy that is not due to alterations in proliferation or apoptosis. Rather, there is an alteration in the extracellular matrix as observed by positive Alcian blue staining and increased collagen by Masson trichrome staining. Microarray analysis of the $PR^{cre/+}SmoM2^{+}$ uteri revealed a chondrocytic signature as well as a number of

genes previously identified as cartilage specific. Previous studies examining bone development established a critical role for Hh signaling in bone formation that includes chondrocyte proliferation and differentiation resulting in the production of a cartilaginous matrix [10]. We have validated a number of these genes as being up-regulated in the $PR^{cre/+}SmoM2^{+}$ uterus, including both signaling molecules shown to be critical for chondrocyte proliferation and differentiation as well as genes that compose the extracellular matrix (Fig. 5). For instance, the mechanism by which Hh signaling promotes bone development has been intimately linked to parathyroid hormone signaling [33]. In the $PR^{cre/+}SmoM2^{+}$ uterus, both the ligand (*Pthlh*) and the receptor (*Pthr1*) are up-regulated, indicating an up-regulation of this signaling pathway (Fig. 5). In addition, we have shown that Hh activation results in increased *Wnt5a* expression, which has been shown to be necessary for bone formation as ablation of *Wnt5a* in mice leads to a defect in bone development [32]. Finally, administration of recombinant BMP2 to mesenchymal stem cells is sufficient to induce differentiation into chondrocytes, and in the 3-mo-old $PR^{cre/+}SmoM2^{+}$ uterus, *Bmp2* expression is significantly increased [30]. Thus, there is great commonality between uterine- and bone-signaling pathways, and activation of SMO in the uterus leads to a chondrocytic phenotype. Furthermore, cultured endometrial stromal cells, both human and bovine, have been shown to exhibit chondrocytic/osteogenic properties, which may occur as a result of a perturbation in endometrial Hh signaling [43, 44]. In addition to demonstrating that Hh activation results in the induction of genes involved in chondrocyte proliferation and differentiation, these data also suggest that SMO activation may be affecting a progenitor cell population as the uterine stromal cells exhibit an altered differentiation profile; additional studies need to be conducted to explore this further.

Furthermore, the idea that activation of SMO in the mouse uterus affects a uterine progenitor cell population is consistent with the observed phenotype of the $PR^{cre/+}SmoM2^{+}$ luminal epithelium. Instead of a simple columnar epithelium, the $PR^{cre/+}SmoM2^{+}$ luminal epithelium also contained a p63-positive basal cell layer (Fig. 3C). Previously, activation of Hh signaling has been implicated in the proliferation and subsequent expansion of p63-positive basal cells in the skin as overexpression of the Hh ligands resulted in increased epidermal p63-positive cell layers [45]. In the female reproductive tract, p63-positive basal cells are localized to the cervix and vagina [46]. They have been observed in the uterus upon in utero exposure to the synthetic estrogen diethylstilbesterol or genetic ablation of the WNT-signaling ligands, *Wnt7a* and *Wnt5a* [47–49]. The mechanism by which Hh signaling is involved in the differentiation of the uterine basal cell layer remains unknown. However, because activation of Hh signaling was only observed in the uterine stroma, this suggests that, as with glandular development, the appearance of basal cells in the $PR^{cre/+}SmoM2^{+}$ uterus may be due to the uterine stroma acting on the luminal epithelium and may also involve an influence of Hh signaling on a progenitor cell population. Elucidating the paracrine factors involved in this stromal-epithelial communication are vital for understanding the development of these basal cells in the uterus.

The ability to investigate the effect of aging on the $PR^{cre/+}SmoM2^{+}$ mice was prevented by the development of rhabdomyosarcomas in the pectoral muscles of the mice (Supplemental Figure S3). Previously, Hh signaling has been implicated in the development of rhabdomyosarcomas as mice that lost a copy of *Ptch* or that experienced inducible SMO activation develop these tumors [34–37]. The presence of this phenotype was surprising as PR^{cre} recombination of floxed alleles has not be observed in the muscle [14]. Thus, the development of these tumors may not be a direct effect of SMO activation in the muscle, but may possibly be due to indirect developmental or paracrine effects from surrounding tissue.

In conclusion, we have demonstrated that constitutive activation of SMO in the murine uterus renders female mice infertile as a result of an inability of ova to be fertilized in vivo and the uterus to exhibit a decidual response. In addition, $PR^{cre/+}SmoM2^{+}$ mice exhibit abnormal uterine development such that there is the appearance of a p63-positive basal cell layer in the luminal epithelium, a reduction in the number of uterine glands, and an alteration of the stromal extracellular matrix. Thus, tight regulation of the Hh-signaling pathway is necessary not only for normal uterine function, but also for proper development of the uterus.

ACKNOWLEDGMENTS

We wish to thank the Baylor College of Medicine Genetically Engineered Mouse Core (Jie Wang, Ruina Zhang, and Dongcai Liang) for assistance with the in vitro fertilization assay. We also thank Jinghua Li, Sungnam Cho, Jie Yang, Yiqun Zhang, and Bryan Ngo for technical assistance and Janet DeMayo, M.S., for manuscript preparation. The SmoM2 mice were kindly provided by Dr. Andrew P. McMahon (Department of Molecular and Cellular Biology, Harvard University, Boston MA).

REFERENCES

1. Yin Y, Ma L. Development of the mammalian female reproductive tract. J Biochem 2005; 137:677–683.
2. Gray CA, Bartol FF, Tarleton BJ, Wiley AA, Johnson GA, Bazer FW, Spencer TE. Developmental biology of uterine glands. Biol Reprod 2001; 65:1311–1323.
3. Gray CA, Taylor KM, Ramsey WS, Hill JR, Bazer FW, Bartol FF, Spencer TE. Endometrial glands are required for preimplantation conceptus elongation and survival. Biol Reprod 2001; 64:1608–1613.
4. Franco HL, Jeong JW, Tsai SY, Lydon JP, DeMayo FJ. In vivo analysis of progesterone receptor action in the uterus during embryo implantation. Semin Cell Dev Biol 2008; 19:178–186.
5. Matsumoto H, Zhao X, Das SK, Hogan BL, Dey SK. Indian hedgehog as a progesterone-responsive factor mediating epithelial-mesenchymal interactions in the mouse uterus. Dev Biol 2002; 245:280–290.
6. Takamoto N, Zhao B, Tsai SY, DeMayo FJ. Identification of Indian hedgehog as a progesterone-responsive gene in the murine uterus. Mol Endocrinol 2002; 16:2338–2348.
7. Varjosalo M, Taipale J. Hedgehog: functions and mechanisms. Genes Dev 2008; 22:2454–2472.
8. Krishnan V, Elberg G, Tsai MJ, Tsai SY. Identification of a novel sonic hedgehog response element in the chicken ovalbumin upstream promoter-transcription factor II promoter. Mol Endocrinol 1997; 11:1458–1466.
9. Krishnan V, Pereira FA, Qiu Y, Chen CH, Beachy PA, Tsai SY, Tsai MJ. Mediation of Sonic hedgehog-induced expression of COUP-TFII by a protein phosphatase. Science 1997; 278:1947–1950.
10. St-Jacques B, Hammerschmidt M, McMahon AP. Indian hedgehog signaling regulates proliferation and differentiation of chondrocytes and is essential for bone formation. Genes Dev 1999; 13:2072–2086.
11. Day TF, Yang Y. Wnt and hedgehog signaling pathways in bone development. J Bone Joint Surg Am 2008; 90(suppl 1):19–24.
12. Long F, Zhang XM, Karp S, Yang Y, McMahon AP. Genetic manipulation of hedgehog signaling in the endochondral skeleton reveals a direct role in the regulation of chondrocyte proliferation. Development 2001; 128:5099–5108.
13. Lee K, Jeong J, Kwak I, Yu CT, Lanske B, Soegiarto DW, Toftgard R, Tsai MJ, Tsai S, Lydon JP, DeMayo FJ. Indian hedgehog is a major mediator of progesterone signaling in the mouse uterus. Nat Genet 2006; 38:1204–1209.
14. Soyal SM, Mukherjee A, Lee KY, Li J, Li H, DeMayo FJ, Lydon JP. Cre-mediated recombination in cell lineages that express the progesterone receptor. Genesis 2005; 41:58–66.
15. Talbi S, Hamilton AE, Vo KC, Tulac S, Overgaard MT, Dosiou C, Le Shay N, Nezhat CN, Kempson R, Lessey BA, Nayak NR, Giudice LC. Molecular phenotyping of human endometrium distinguishes menstrual

cycle phases and underlying biological processes in normo-ovulatory women. Endocrinology 2006; 147:1097–1121.
16. Burney RO, Talbi S, Hamilton AE, Vo KC, Nyegaard M, Nezhat CR, Lessey BA, Giudice LC. Gene expression analysis of endometrium reveals progesterone resistance and candidate susceptibility genes in women with endometriosis. Endocrinology 2007; 148:3814–3826.
17. Kurihara I, Lee DK, Petit FG, Jeong J, Lee K, Lydon JP, DeMayo FJ, Tsai MJ, Tsai SY. COUP-TFII mediates progesterone regulation of uterine implantation by controlling ER activity. PLoS Genet 2007; 3:e102.
18. Takamoto N, Kurihara I, Lee K, Demayo FJ, Tsai MJ, Tsai SY. Haploinsufficiency of chicken ovalbumin upstream promoter transcription factor II in female reproduction. Mol Endocrinol 2005; 19:2299–2308.
19. Xie J, Murone M, Luoh SM, Ryan A, Gu Q, Zhang C, Bonifas JM, Lam CW, Hynes M, Goddard A, Rosenthal A, Epstein EH Jr, de Sauvage FJ. Activating Smoothened mutations in sporadic basal-cell carcinoma. Nature 1998; 391:90–92.
20. Jeong J, Mao J, Tenzen T, Kottmann AH, McMahon AP. Hedgehog signaling in the neural crest cells regulates the patterning and growth of facial primordia. Genes Dev 2004; 18:937–951.
21. Hogan B, Costantini F, Lacy E. Manipulating the mouse embryo: a laboratory manual. Cold Spring Harbor, NY: Cold Spring Harbor Laboratory, 1986.
22. Finn CA, Martin L. Endocrine control of the timing of endometrial sensitivity to a decidual stimulus. Biol Reprod 1972; 7:82–86.
23. Goodrich LV, Milenkovic L, Higgins KM, Scott MP. Altered neural cell fates and medulloblastoma in mouse patched mutants. Science 1997; 277: 1109–1113.
24. Soriano P. Generalized lacZ expression with the ROSA26 Cre reporter strain. Nat Genet 1999; 21:70–71.
25. Creighton CJ, Casa A, Lazard Z, Huang S, Tsimelzon A, Hilsenbeck SG, Osborne CK, Lee AV. Insulin-like growth factor-I activates gene transcription programs strongly associated with poor breast cancer prognosis. J Clin Oncol 2008; 26:4078–4085.
26. Dennis G Jr, Sherman BT, Hosack DA, Yang J, Gao W, Lane HC, Lempicki RA. DAVID: database for annotation, visualization, and integrated discovery. Genome Biol 2003; 4:P3.
27. Huang da W, Sherman BT, Lempicki RA. Systematic and integrative analysis of large gene lists using DAVID bioinformatics resources. Nat Protoc 2009; 4:44–57.
28. Besnard V, Wert SE, Hull WM, Whitsett JA. Immunohistochemical localization of Foxa1 and Foxa2 in mouse embryos and adult tissues. Gene Expr Patterns 2004; 5:193–208.
29. McCluggage WG, Sumathi VP, Maxwell P. CD10 is a sensitive and diagnostically useful immunohistochemical marker of normal endometrial stroma and of endometrial stromal neoplasms. Histopathology 2001; 39: 273–278.
30. Mrugala D, Dossat N, Ringe J, Delorme B, Coffy A, Bony C, Charbord P, Haupl T, Daures JP, Noel D, Jorgensen C. Gene expression profile of multipotent mesenchymal stromal cells: identification of pathways common to TGFbeta3/BMP2-induced chondrogenesis. Cloning Stem Cells 2009; 23:711–723.
31. Funari VA, Day A, Krakow D, Cohn ZA, Chen Z, Nelson SF, Cohn DH. Cartilage-selective genes identified in genome-scale analysis of non-cartilage and cartilage gene expression. BMC Genomics 2007; 8:165.
32. Yang Y, Topol L, Lee H, Wu J. Wnt5a and Wnt5b exhibit distinct activities in coordinating chondrocyte proliferation and differentiation. Development 2003; 130:1003–1015.
33. Lai LP, Mitchell J. Indian hedgehog: its roles and regulation in endochondral bone development. J Cell Biochem 2005; 96:1163–1173.
34. Aszterbaum M, Epstein J, Oro A, Douglas V, LeBoit PE, Scott MP, Epstein EH Jr. Ultraviolet and ionizing radiation enhance the growth of BCCs and trichoblastomas in patched heterozygous knockout mice. Nat Med 1999; 5:1285–1291.
35. Corcoran RB, Scott MP. A mouse model for medulloblastoma and basal cell nevus syndrome. J Neurooncol 2001; 53:307–318.
36. Hahn H, Wojnowski L, Zimmer AM, Hall J, Miller G, Zimmer A. Rhabdomyosarcomas and radiation hypersensitivity in a mouse model of Gorlin syndrome. Nat Med 1998; 4:619–622.
37. Mao J, Ligon KL, Rakhlin EY, Thayer SP, Bronson RT, Rowitch D, McMahon AP. A novel somatic mouse model to survey tumorigenic potential applied to the Hedgehog pathway. Cancer Res 2006; 66:10171–10178.
38. Ren Y, Cowan RG, Harman RM, Quirk SM. Dominant activation of the hedgehog signaling pathway in the ovary alters theca development and prevents ovulation. Mol Endocrinol 2009; 11:61–76.
39. Suarez SS, Pacey AA. Sperm transport in the female reproductive tract. Hum Reprod Update 2006; 12:23–37.
40. Stewart CL, Kaspar P, Brunet LJ, Bhatt H, Gadi I, Kontgen F, Abbondanzo SJ. Blastocyst implantation depends on maternal expression of leukaemia inhibitory factor. Nature 1992; 359:76–79.
41. Chen JR, Cheng JG, Shatzer T, Sewell L, Hernandez L, Stewart CL. Leukemia inhibitory factor can substitute for nidatory estrogen and is essential to inducing a receptive uterus for implantation but is not essential for subsequent embryogenesis. Endocrinology 2000; 141:4365–4372.
42. Bartol FF, Wiley AA, Coleman DA, Wolfe DF, Riddell MG. Ovine uterine morphogenesis: effects of age and progestin administration and withdrawal on neonatal endometrial development and DNA synthesis. J Anim Sci 1988; 66:3000–3009.
43. Donofrio G, Franceschi V, Capocefalo A, Cavirani S, Sheldon IM. Bovine endometrial stromal cells display osteogenic properties. Reprod Biol Endocrinol 2008; 6:65.
44. Wolff EF, Wolff AB, Hongling D, Taylor HS. Demonstration of multipotent stem cells in the adult human endometrium by in vitro chondrogenesis. Reprod Sci 2007; 14:524–533.
45. Adolphe C, Narang M, Ellis T, Wicking C, Kaur P, Wainwright B. An in vivo comparative study of sonic, desert and Indian hedgehog reveals that hedgehog pathway activity regulates epidermal stem cell homeostasis. Development 2004; 131:5009–5019.
46. Kurita T, Cunha GR, Robboy SJ, Mills AA, Medina RT. Differential expression of p63 isoforms in female reproductive organs. Mech Dev 2005; 122:1043–1055.
47. Kurita T, Mills AA, Cunha GR. Roles of p63 in the diethylstilbestrol-induced cervicovaginal adenosis. Development 2004; 131:1639–1649.
48. Mericskay M, Kitajewski J, Sassoon D. Wnt5a is required for proper epithelial-mesenchymal interactions in the uterus. Development 2004; 131:2061–2072.
49. Miller C, Sassoon DA. Wnt-7a maintains appropriate uterine patterning during the development of the mouse female reproductive tract. Development 1998; 125:3201–3211.